Biosensors and Bioelectronics 144 (2019) 111674

Contents lists available at ScienceDirect

Biosensors and Bioelectronics

journal homepage: www.elsevier.com/locate/bios

An ultrasensitive electrochemical sensing method for detection of microcystin-LR based on infinity-shaped DNA structure using double aptamer and terminal deoxynucleotidyl transferase

Khalil Abnous[a,b,1], Noor Mohammad Danesh[c,1], Morteza Alinezhad Nameghi[a], Mohammad Ramezani[a], Mona Alibolandi[a], Parirokh Lavaee[d], Seyed Mohammad Taghdisi[e,f,*]

[a] Pharmaceutical Research Center, Pharmaceutical Technology Institute, Mashhad University of Medical Sciences, Mashhad, Iran
[b] Department of Medicinal Chemistry, School of Pharmacy, Mashhad University of Medical Sciences, Mashhad, Iran
[c] Research Institute of Sciences and New Technology, Mashhad, Iran
[d] Academic Center for Education, Culture and Research, Research Institute for Industrial Biotechnology, Industrial Biotechnology on Microorganisms, Mashhad, Iran
[e] Targeted Drug Delivery Research Center, Pharmaceutical Technology Institute, Mashhad University of Medical Sciences, Mashhad, Iran
[f] Department of Pharmaceutical Biotechnology, School of Pharmacy, Mashhad University of Medical Sciences, Mashhad, Iran

ARTICLE INFO

Keywords:
Infinity-shape
MC-LR
Electrochemical sensing platform
Real sample
TdT

ABSTRACT

This study develops a novel electrochemical sensing platform for microcystin-LR (MC-LR) detection. This aptasensor comprises the hybridization of double aptamer to its complementary strand (CS) on the surface of electrode and generation of an Infinity-shaped DNA structure in the absence of target by terminal deoxynucleotidyl transferase (TdT). The formation of Infinity-shaped construction leads to the development of an ultrasensitive aptasensor for MC-LR detection. In the presence of MC-LR, double aptamer is dissociated from its CS because of its high affinity for MC-LR and leaves the surface of electrode. Subsequently, no Infinity-shaped structure is formed following the introduction of TdT and a strong current signal is observed. The proposed method was employed for specific detection of MC-LR in the range from 60 pM to 1000 nM with a detection limit of 15 pM. The credibility of the approach was confirmed by detection of MC-LR in real samples like serum and tap water samples. This study provides a new aptasensor for detection of MC-LR as well as other toxin analysis.

1. Introduction

Microcystins, released by cyanobacteria in water environment, are a group of cyclic hepta-peptide toxins (Guan et al., 2019; Zhang et al., 2018b). Microcystin-LR (MC-LR) is the most toxic and common variant among different microcystin congeners (Liu et al., 2019a; Zhang et al., 2018c). MC-LR is considered as a great threat to human health which can lead to liver damage and even tumor promotion through consumption of polluted food products and drinking water (He et al., 2019b; Yang et al., 2018). The results have shown that the presence of microcystins in serum samples in the range of below 1 ng/mL to 10 ng/mL can cause acute liver injuries (Welten et al., 2019). Thus, it is of great importance to introduce reliable analytical approaches with high sensitivity for MC-LR detection.

Different laboratory techniques for detection of MC-LR have been introduced including capillary electrophoresis (Tong et al., 2010), high-performance liquid chromatography (HPLC) (Ma et al., 2015), immunoassay (Hou et al., 2016) and liquid chromatography-mass spectrometry (LC-MS) (Zastepa et al., 2015). However, although these approaches are sensitive, they usually need skilled operators, large and expensive instruments and complicated analytical procedures (He et al., 2019a; Tang et al., 2018; Zhang et al., 2019c). Thus, development of alternative sensing methods to circumvent these problems are highly needed.

Nowadays, nucleic acid aptamers have obtained a great potential for development of selective and sensitive biosensors. Aptamers are short single-stranded nucleic acids which can tightly bind to their target molecules with high sensitivity (Li et al., 2019; Taghdisi et al., 2018). They are isolated from random nucleic acid libraries via an *in vitro* method called as Systematic Evolution of Ligands by EXponential enrichment (SELEX) (Yang et al., 2019). Compared to antibodies, aptamers offer several prominent characteristics including simple and ease

* Corresponding author. Targeted Drug Delivery Research Center, Pharmaceutical Technology Institute, Mashhad University of Medical Sciences, Mashhad, Iran.
E-mail address: taghdisihm@mums.ac.ir (S.M. Taghdisi).
[1] These authors contributed equally to the work.

https://doi.org/10.1016/j.bios.2019.111674
Received 21 August 2019; Accepted 3 September 2019
Available online 05 September 2019
0956-5663/

of synthesis, batch-to-batch uniformity, ease of labeling, low cost and high stability (Hao et al., 2019; Saberi et al., 2019).

Electrochemical method is an attractive approach for bioanalysis owing to its feasibility of miniaturization, simple equipment, ease of operation and low cost (Fan et al., 2019; He and Yan, 2019; Nameghi et al., 2019).

Herein, an ultrasensitive detection platform was developed for MC-LR detection based on Infinity-shaped DNA structure and terminal deoxynucleotidyl transferase (TdT). Until now, various electrochemical aptasensors with diverse shapes have been proposed by our team, such as ladder-shape (Taghdisi et al., 2019), M-shape (Taghdisi et al., 2016) and π-shape (Abnous et al., 2017a). The developed sensing method has a simple design compared to these aptasensors because it has been composed of only two kinds of sequences, complementary strand of aptamer (CS) and MC-LR aptamer (Liu et al., 2019a; Zhang et al., 2019c). Also, it has the characteristic of high sensitivity like these approaches because in the presence of MC-LR, double aptamer leaves its CS and the surface of electrode, resulting in more entry of redox marker ($[Fe(CN)_6]^{3-/4-}$) to the electrode surface. While, in the lack of MC-LR, the Infinity-shaped structure is formed in the surface of electrode and the redox marker has very less connection with the electrode surface.

2. Materials and methods

2.1. Materials

Oligonucleotide sequences were ordered from Microsynth (Switzerland, Table S1). Microcystin-LR (MC-LR), Tris(2-carboxyethyl) phosphine hydrochloride (TCEP), microcystin-LA (MC-LA), potassium hexacyanoferrate(III) ($K_3[Fe(CN)_6]$), atrazine, 6-mercaptohexanol (MCH), acetamiprid, zearalenone, potassium hexacyanoferrate(II) trihydrate ($K_4[Fe(CN)_6].3H_2O$), and aflatoxin M1 (AFM1) were purchased from Sigma-Aldrich (USA). Terminal deoxynucleotidyl transferase (TdT) was obtained from Thermo Fisher Scientific (USA). MC-LR ELISA kit was obtained from MyBioSource (USA).

2.2. Instruments and electrochemical measurements

The electrochemical studies were performed with a μSTAT 400 portable BiPotentiostat/Galvanostat (DropSens, Spain) using DropView8400 software and screen-printed gold electrodes with gold working electrode (4 mm diameter), silver reference electrode and gold counter electrode (SPGEs, DRP-C220BT, DropSens, Spain).

The electrochemical measurements were performed in 3 mM $[Fe(CN)_6]^{3-/4-}$ and 0.1 M KCl. Cyclic voltammetry (CV) measurements were carried out at the scanning potential from −0.46–0.8 V with a scan rate of 50 mV/s. Differential pulse voltammetry (DPV) was scanned from 0.05 to 0.23 V with a pulse potential of 10 mV and pulse time of 25 ms.

The morphology and the roughness of SPGEs were characterized by scanning electron microscopy (SEM, TESCAN MIRA3 microscope, Czech Republic) and atomic force microscopy (AFM, JPK NanoWizard II microscope, Germany), respectively.

2.3. Construction of the aptasensor and measurement performance of MC-LR

Thiol-modified CS (400 nM final concentration) was mixed with TCEP in 10 mM Tris-HCl buffer (5 mM TCEP, 1 mM EDTA, 100 mM NaCl, pH 7.4) for 1 h to reduce disulfide bond of CS. The reduced CS (10 μL, 400 nM) was incubated on the surface of SPGE and kept for 12 h at room temperature in a moisture-saturated situation to allow CS immobilization on the surface of SPGE. Then, 800 nM double aptamer (10 μL) was dropped on the electrode surface and incubated for 2.5 h at room temperature to be hybridized to its CS. Subsequently, 0.4 mM MCH (10 μL) was dropped on the modified electrode for 1 h to block the blank sites.

For sensing experiment, the double aptamer-CS modified electrodes were incubated with diverse amounts of MC-LR (0–1500 nM) prepared in 5 mM phosphate buffer saline (PBS, pH 7.4) for 60 min at room temperature. After rinsing the electrode with 5 mM PBS, 8 U TdT, 10 mM dTTP and 1X TdT reaction buffer were placed on the surface of electrode for 90 min at 37 °C and further analyzed using DPV analysis.

2.4. Interference study of the sensing method

To assess the specificity of the proposed approach, the aptasensor was incubated with 1000 nM MC-LR and other toxins like MC-LA, atrazine, acetamiprid, zearalenone and AFM1 with the same concentration, followed by DPV measurements.

2.5. Tap water and serum sample analysis

Various amounts of MC-LR (0–1500 nM) were spiked into tap water and 10-fold diluted serum samples and the presence of MC-LR was investigated by the sensing approach and DPV analysis.

3. Results and discussion

3.1. Mechanism of MC-LR sensing

In the present study, an electrochemical aptasensor was developed for MC-LR detection based on double aptamer-CS hybridization and TdT enzyme to elongate the double aptamer and form the Infinity-shaped DNA construction on the electrode surface. TdT is a DNA polymerase which catalyzes the template-independent addition of deoxyribonucleoside triphosphates (dNTPs) to 3′-OH terminus of ssDNAs or dsDNAs (Que et al., 2019; Wang et al., 2019).

The detection procedure developed in this research is shown in Scheme 1. Without introduction of MC-LR, a poly-T tail is added to the 3′-end of double aptamer by TdT, resulting in the hybridization between poly-T tail and poly-A tail of 3′-end of double aptamer and formation of the Infinity-shaped DNA structure on the electrode surface which repels the $[Fe(CN)_6]^{3-/4-}$ anions from the electrode surface by both its activity as a physical barrier to the electron transfer procedure and electrostatic repulsion between the redox probe and the negatively charged phosphate backbone of the Infinity-shaped construction. Thus, this phenomenon leads to a weak peak current.

Upon addition of MC-LR, the aptamer-MC-LR conjugate leaves the surface of electrode because the affinity between aptamer-target is stronger than the aptamer-complementary strand (Zhang et al. 2019a, 2019b). Therefore, in the presence of TdT, no DNA elongation occurs in the electrode surface and the redox current increases due to an elevation on electron transfer capability between the surface of electrode and redox marker.

3.2. Optimization of the aptasensor reaction conditions

3.2.1. Effect of concentration of TdT

The concentration of TdT, one of the main parameters which can affect the response of aptasensor, was evaluated. From Fig. 1(a), it is clearly found that in the absence of MC-LR, the relative electrochemical response enhances with the increase of concentration of TdT and it remains stable when the amount of TdT is 8 U. So, 8 U TdT was the suitable concentration for the subsequent experiments.

3.2.2. Effect of incubation time of MC-LR

The reaction time of target is another important parameter affecting the response of sensing method. As shown in Fig. 1(b), the results exhibited that the relative electrochemical signal of the biosensor increased with the enhancement of reaction time of MC-LR from 10 to 60 min and after that, the response was stable. Thus, the reaction time of 60 min was chosen for subsequent tests.

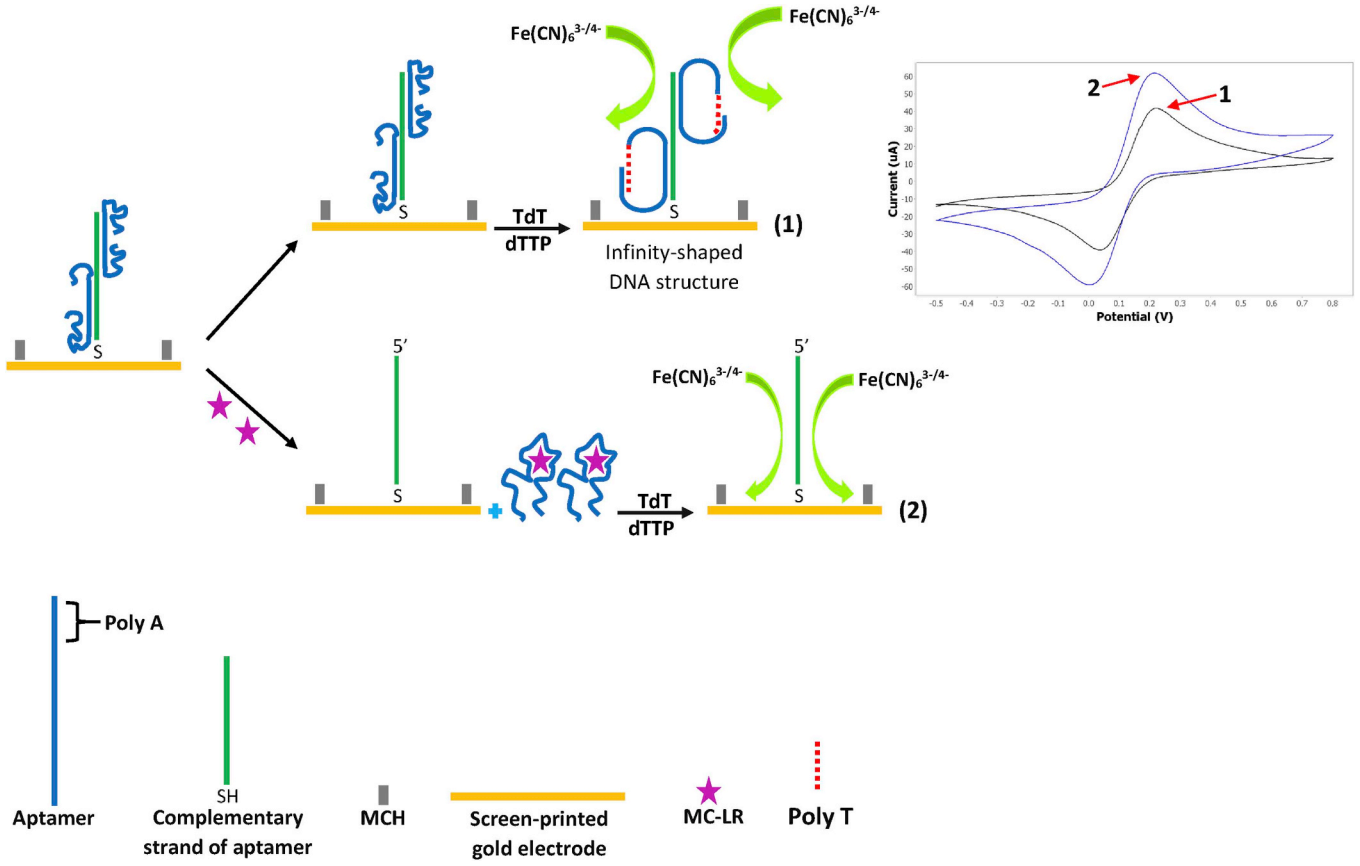

Scheme 1. Illustration of the electrochemical biosensor fabrication and the mechanism for detection of MC-LR.

3.3. Characterization of the sensing approach fabrication and operation

For the electrochemical characterization, CV was employed to verify the fabrication procedure of the modified electrode and the aptasensor performance. As shown in Fig. 2 (a), the current signal indicated a significant decrease compared to bare electrode (red curve, a curve) when thiol-modified CS was placed on the surface of SPGE (pink curve, b curve). This is due to weak conductivity of CS and its negative charge characteristic, decreasing the electron transfer. When the modified electrode was incubated with double aptamer, a further decrease in peak current was observed (green curve, e curve). This was owing to the increase of the negative charge on the surface of electrode produced by double aptamer-CS modified electrode and confirmed the successful attachment of double aptamer to its CS. In the absence of MC-LR, the redox current was further declined after treatment of the electrode with TdT and dTTP (black curve, f curve) which was ascribed to the formation of the Infinity-shaped construction as a physical hurdle with more negative charge on the electrode surface, hindering further the electron transfer. When the double aptamer-CS modified electrode was incubated with MC-LR, CV curve significantly increased because of the release of aptamer-MC-LR conjugate from the electrode surface and reduction of hindrance (gray curve, c curve). As expected, the CV response did not change after treatment with TdT and dTTP (blue curve, d curve) because there was no free 3′-end of ssDNA or dsDNA on the surface of electrode to be elongated by TdT.

Also, the modification of electrode with CS was examined by SEM and AFM tests. AFM images exhibited that the roughness of electrode raised from 298.7 to 355.9 nm, following the treatment of the electrode with thiol-modified CS (Fig. S1). Furthermore, after incubation with CS, an obvious morphology change of electrode was observed from SEM images (Fig. 2(b) and (c)). According to these results, it is clear that the CS has been successfully immobilized on the electrode surface.

The fabrication and function of the presented biosensor was also evaluated via agarose gel electrophoresis (Fig. S2). Only one band with lower mobility shift appeared (lane 2) following the incubation of aptamer with CS, confirming the successful hybridization of aptamer with its CS and formation of double aptamer-CS structure. In the presence of MC-LR (1000 nM), the double aptamer-CS structure was disassembled (lane 1), offering the good performance of the sensing method for its target.

3.4. Quantification of MC-LR

Under the optimal conditions, DPV was employed to measure the MC-LR concentrations. Fig. 3(a) indicates the electrochemical responses of the aptasensor in the presence of different amounts of MC-LR. As expected, with the increasing amount of MC-LR, the redox peak increased. The aptasensor showed a wide linear relationship towards MC-LR with a linear range of 60 pM–1000 nM (0.0597–995.189 μg/L) (Fig. 3(b)). Also, the limit of detection (LOD) and limit of quantification (LOQ) of the sensing method were determined to be 15 pM (0.0149 μg/L, S/N = 3) and 60 pM (0.0597 μg/L, S/N = 10), respectively. The obtained LOD is better than or comparable to the other reported analytical methods for MC-LR detection (Table 1) (Abnous et al., 2017b; He et al., 2018; Li et al., 2018; Liu et al., 2019b; Taghdisi et al., 2017; Wu et al., 2019; Zhang et al., 2018a).

3.5. The selectivity study

Cross-reactivity evaluation is a main parameter in sensor assessment. To check the specificity of the presented sensing approach, the relative electrochemical signal of the biosensor towards a variety of interfering toxins was investigated. As displayed in Fig. 3(c) and (d), the relative electrochemical response and DPV response for MC-LR were

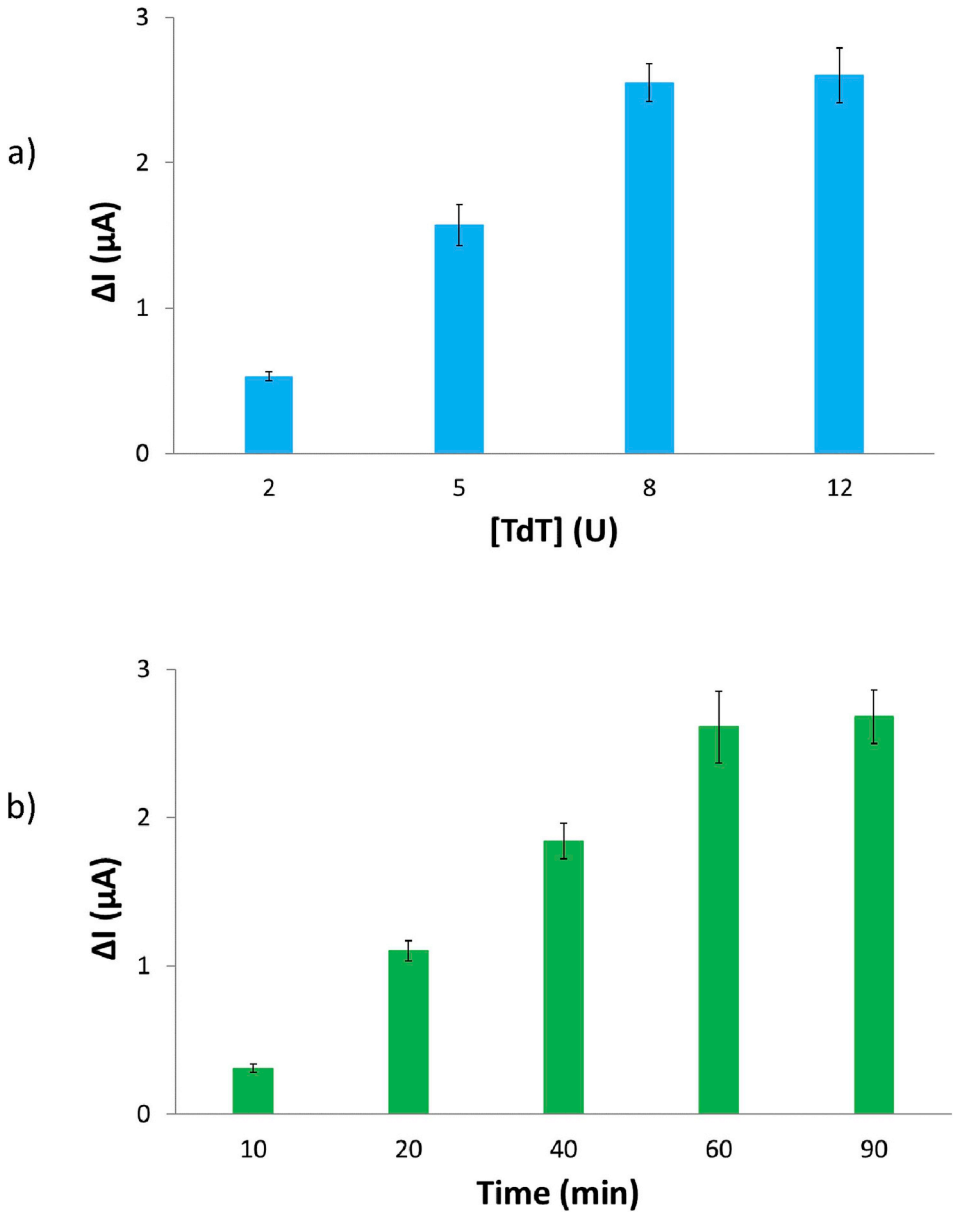

Fig. 1. Optimization tests. (a) The relative electrochemical signal changes (I_0 - I) in response to different concentrations of TdT in the absence of MC-LR. I_0 and I are the current signals before and after addition of TdT. (b) The relative electrochemical signal changes (I - I_0) in response to different incubation times of MC-LR (1000 nM). I_0 and I are the current signals before and after addition of MC-LR.

much greater relative to other examined toxins such as MC-LA, atrazine, acetamiprid, zearalenone and AFM1, suggesting high selectivity of the aptasensor.

3.6. MC-LR analysis in tap water and serum samples

To analyze the application feasibility of the designed method for detecting MC-LR in real samples, the experiments were performed for determination of MC-LR in tap water and serum sample as a complex biological sample. The LODs were measured to be 20 pM (0.0199 μg/L) and 35 pM (0.0348 μg/L) for tap water and serum samples, respectively. Also, the linear relationships were obtained in the range from 70 pM to 900 nM and 100 pM to 750 nM for tap water and serum samples, respectively (Fig. S3). The LOD obtained from the presented approach is much lower than the maximum permitted level of 1 μg/L of MC-LR in drinking water set up by the World Health Organization (WHO) (Guan et al., 2019).

To further confirm the detection accuracy of the developed biosensor, recovery assay was employed for spiked serum samples. The recoveries ranged from 88.6% to 103.2% and relative standard deviations (RSDs) were lower than 5.5% (Table 2), verifying that the presented aptasensor has high accuracy and reproducibility for MC-LR detection in serum samples.

3.7. Stability of the aptasensor

Evaluation of the long-term stability of the sensing method showed a loss of about 2.7% in response (n = 3) when the presented analytical approach was applied for detection of 100 nM MC-LR by the double aptamer-CS modified electrodes which have been kept at 4 °C for 18 days (Fig. S4). This result demonstrated high stability of the developed aptasensor.

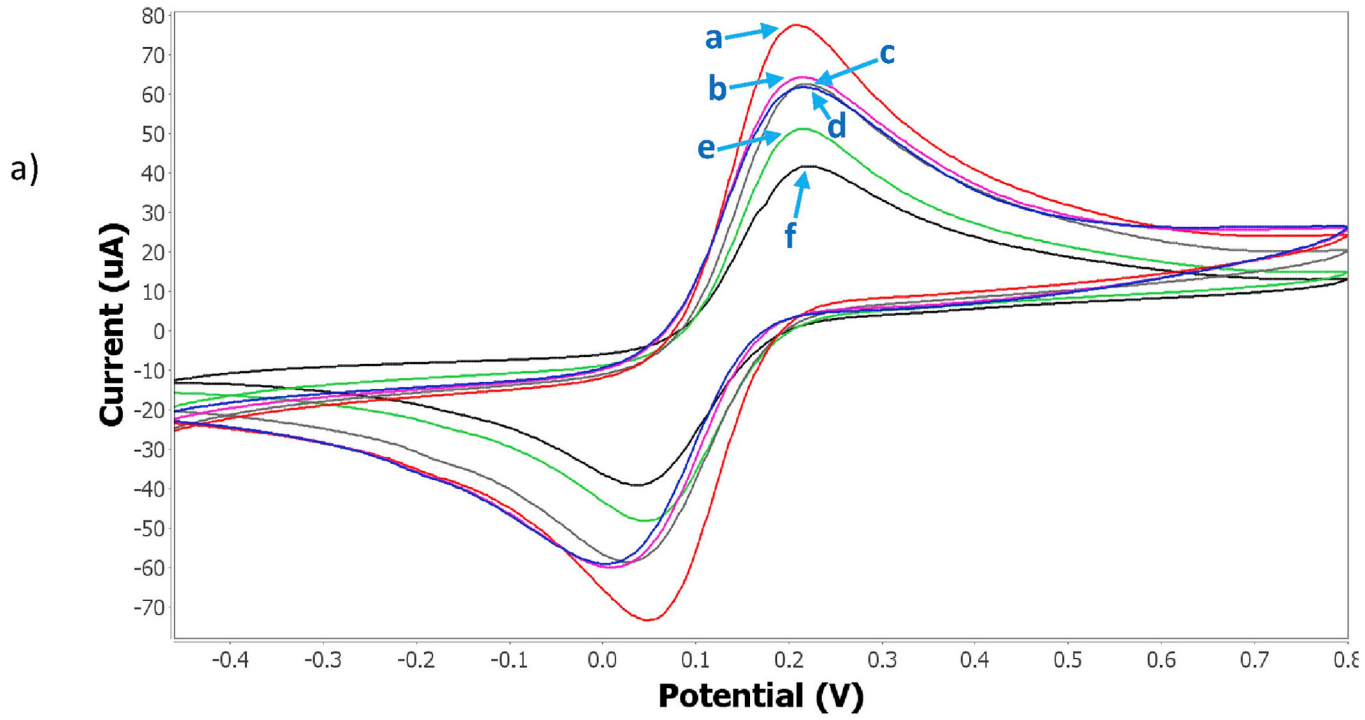

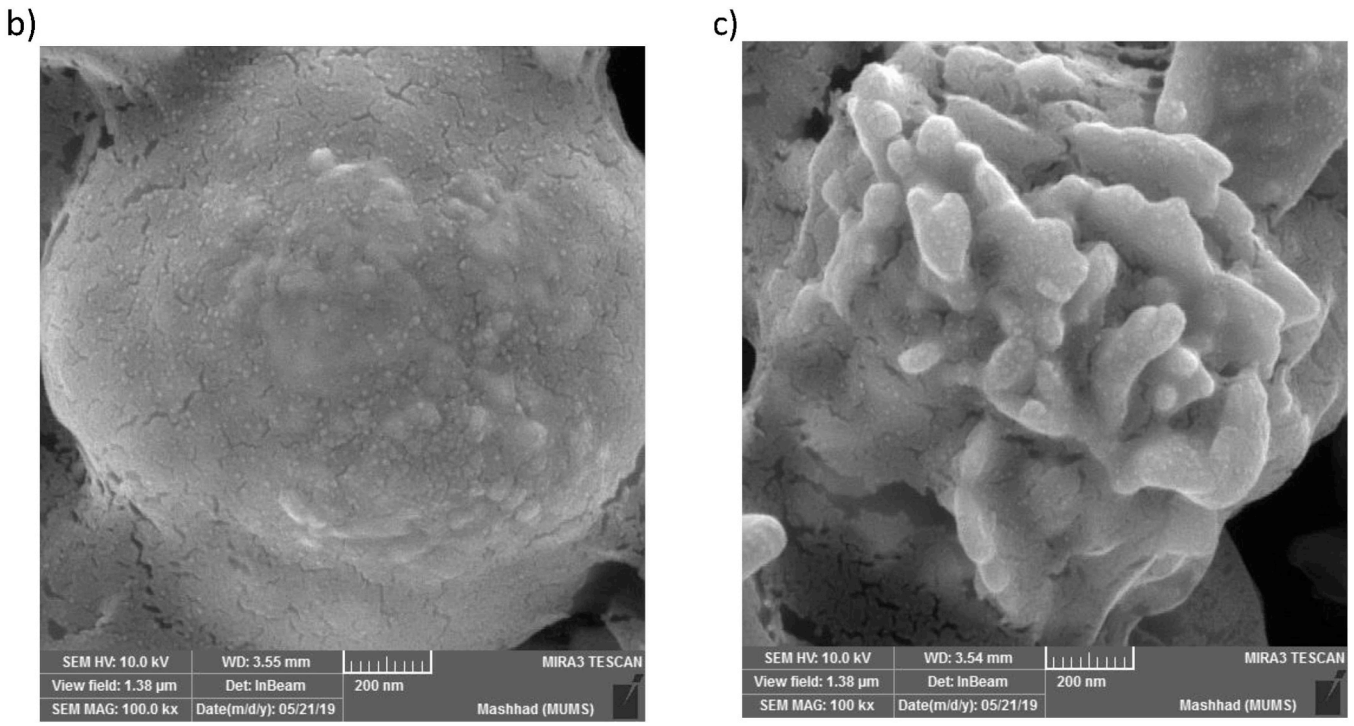

Fig. 2. (a) Electrochemical evaluation of the sensing platform fabrication and performance. Bare electrode (red curve, a curve), CS-modified electrode (pink curve, b curve), double aptamer–CS–modified electrode (green curve, e curve), double aptamer–CS–modified electrode + TdT (Infinity-shaped structure) (black curve, f curve), double aptamer–CS–modified electrode + MC-LR (gray curve, c curve), double aptamer–CS–modified electrode + MC-LR + TdT (blue curve, d curve). (b) SEM image of surface morphology of bare gold electrode. (c) SEM image of surface morphology of modified electrode with CS. (For interpretation of the references to colour in this figure legend, the reader is referred to the Web version of this article.)

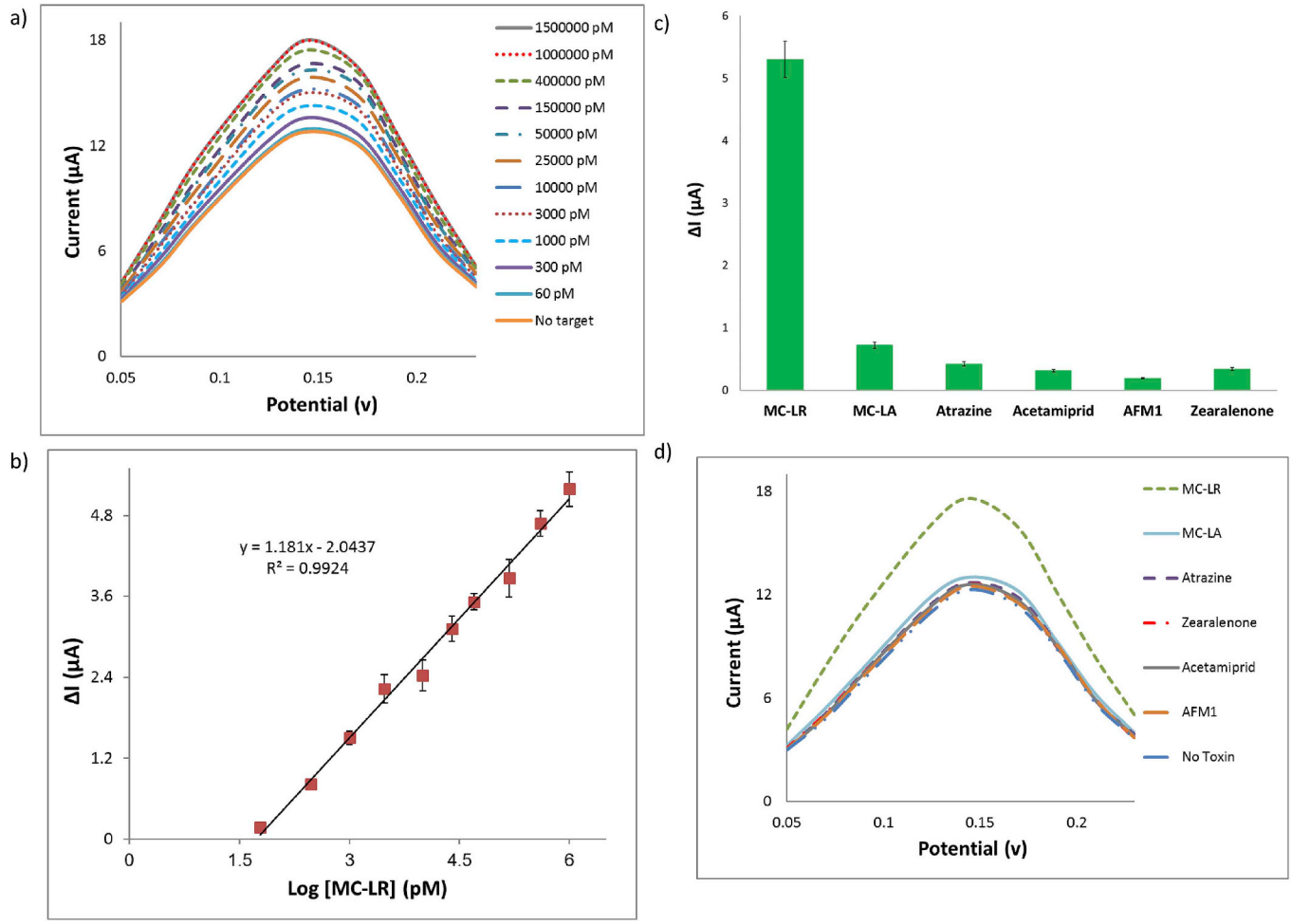

Fig. 3. (a) DPV response of the aptasensor after adding various concentrations of MC-LR (0–1500 nM). (b) Response curve of the relative electrochemical response ($I–I_0$) for MC-LR quantification. I_0 and I are the currents before and after addition of MC-LR, respectively. (c) Selectivity test. The relative electrochemical signal changes ($I–I_0$) of the aptasensor in response to different toxins, including MC-LR, MC-LA, atrazine, acetamiprid, zearalenone and AFM1. I_0 and I are the currents before and after addition of each toxin. (d) DPV response of the aptasensor after treatments with different toxins.

Table 1
Comparison of the proposed aptasensor with other reported MC-LR sensing approaches.

Method	LOD	Linear range	Reference
Label-free aptamer-based detection of MC-LR using a microcantilever array biosensor	1 µg/L	1–50 µg/L	Zhang et al. (2018a)
A fluorescent aptasensor for detection of MC-LR based on single-walled carbon nanotubes and dapoxyl	~0.137 µg/L	~0.398–1194.24 µg/L	Taghdisi et al. (2017)
Colorimetric determination of the MC-LR based on the use of a hairpin aptamer, graphene oxide, and Methylene Blue	~0.217 µg/L	~0.646–995.2 µg/L	Abnous et al. (2017b)
Label-free sensitive detection of MC-LR via aptamer-conjugated gold nanoparticles based on solid-state nanopores	~0.099 µg/L	~0.099–19904 µg/L	He et al. (2018)
Detection of MC-LR with gold immunochromatographic assay assisted by a molecular imprinting technique	0.04 µg/L	0.1–100 µg/L	Wu et al. (2019)
Development of a two-step immunochromatographic assay for MC-LR based on fluorescent microspheres	0.0542 µg/L	0.1–5 µg/L	Liu et al. (2019b)
A shotgun method for high throughput screening microcystins in Margarya melanioides on a triple quadrupole tandem mass spectrometry	0.2 µg/L	2–500 µg/L	Li et al. (2018)
Our electrochemical aptasensor	0.0149 µg/L	0.0597–995.189 µg/L	Current study

Table 2
Recovery of MC-LR from serum samples (n = 4). Data are mean ± relative standard deviation (RSD). 30 and 500 nM concentrations of MC-LR were out of the detection range of ELISA kit.

Serum samples	Added MC-LR (nM)	Found using aptasensor (nM)	Found using ELISA kit (nM)	Recovery (%) ± RSD (%, n = 4) for aptasensor	Recovery (%) ± RSD (%, n = 4) for ELISA kit
1	0.2	0.18	0.19	90 ± 4.2	95 ± 6
2	1	0.98	0.94	98 ± 5.5	94 ± 4.5
3	30	26.58	–	88.6 ± 1.3	–
4	500	516	–	103.2 ± 4	–

4. Conclusion

In conclusion, a novel electrochemical sensing approach was presented for detection of MC-LR employing the Infinity-shaped DNA structure and TdT enzyme. The presence of Infinity-shaped construction led to high sensitivity of the aptasensor. In addition, in comparison with the other shape-based electrochemical aptasensors like ladder-shape or M-shape whose assemblies are complicated and need a lot of sequences, this Infinity-shaped sensor has a simple design and need only two kinds of sequences, aptamer and its CS. The sensing method displayed a very low detection limit, high specificity and a wide linear range for MC-LR. Furthermore, the aptasensor showed satisfactory detection results in the real sample analysis. However, the application of TdT enzyme increases the cost and time of target detection. This study suggests a new strategy for detection of MC-LR and can provide potential uses for other toxins detection.

Declaration of competing interest

The authors declare that they have no known competing financial interests or personal relationships that could have appeared to influence the work reported in this paper.

Acknowledgment

Financial support of this study was provided by Mashhad University of Medical Sciences.

Appendix A. Supplementary data

Supplementary data to this article can be found online at https://doi.org/10.1016/j.bios.2019.111674.

References

Abnous, K., Danesh, N.M., Alibolandi, M., Ramezani, M., Sarreshtehdar Emrani, A., Zolfaghari, R., Taghdisi, S.M., 2017a. A new amplified π-shape electrochemical aptasensor for ultrasensitive detection of aflatoxin B1. Biosens. Bioelectron. 94, 374–379.

Abnous, K., Danesh, N.M., Ramezani, M., Taghdisi, S.M., 2017b. Colorimetric determination of the microcystin leucine-arginine based on the use of a hairpin aptamer, graphene oxide, and Methylene Blue acting as an optical probe. Microchimica Acta 184 (11), 4451–4457.

Fan, L., Zhang, C., Yan, W., Guo, Y., Shuang, S., Dong, C., Bi, Y., 2019. Design of a facile and label-free electrochemical aptasensor for detection of atrazine. Talanta 201, 156–164.

Guan, T., Huang, W., Xu, N., Xu, Z., Jiang, L., Li, M., Wei, X., Liu, Y., Shen, X., Li, X., Yi, C., Lei, H., 2019. Point-of-need detection of microcystin-LR using a smartphone-controlled electrochemical analyzer. Sens. Actuators B Chem. 294, 132–140.

Hao, Z., Pan, Y., Shao, W., Lin, Q., Zhao, X., 2019. Graphene-based fully integrated portable nanosensing system for on-line detection of cytokine biomarkers in saliva. Biosens. Bioelectron. 134, 16–23.

He, B., Yan, X., 2019. A "signal-on" voltammetric aptasensor fabricated by hcPt@AuNFs/PEI-rGO and Fe_3O_4 NRs/rGO for the detection of zearalenone. Sens. Actuators B Chem. 290, 477–483.

He, D., Wu, Z., Cui, B., Jin, Z., 2019a. A novel SERS-based aptasensor for ultrasensitive sensing of microcystin-LR. Food Chem. 278, 197–202.

He, F., Liang, L., Zhou, S., Xie, W., He, S., Wang, Y., Tlili, C., Tong, S., Wang, D., 2018. Label-free sensitive detection of microcystin-LR via aptamer-conjugated gold nanoparticles based on solid-state nanopores. Langmuir 34 (49), 14825–14833.

He, Z., Cai, Y., Yang, Z., Li, P., Lei, H., Liu, W., Liu, Y., 2019b. A dual-signal readout enzyme-free immunosensor based on hybridization chain reaction-assisted formation of copper nanoparticles for the detection of microcystin-LR. Biosens. Bioelectron. 126, 151–159.

Hou, L., Ding, Y., Zhang, L., Guo, Y., Li, M., Chen, Z., Wu, X., 2016. An ultrasensitive competitive immunosensor for impedimetric detection of microcystin-LR via antibody-conjugated enzymatic biocatalytic precipitation. Sens. Actuators B Chem. 233, 63–70.

Li, J., Wang, S., Jiang, B., Xiang, Y., Yuan, R., 2019. Target-induced structure switching of aptamers facilitates strand displacement for DNAzyme recycling amplification detection of thrombin in human serum. Analyst 144 (7), 2430–2435.

Li, S., Cui, Y., Wang, Y., Dai, Z., Shen, Q., 2018. A shotgun method for high throughput screening microcystins in Margarya melanioides on a triple quadrupole tandem mass spectrometry. Food Chem. 269, 89–95.

Liu, X., Tang, Y., Liu, P., Yang, L., Li, L., Zhang, Q., Zhou, Y., Khan, M.Z.H., 2019a. A highly sensitive electrochemical aptasensor for detection of microcystin-LR based on a dual signal amplification strategy. Analyst 144 (5), 1671–1678.

Liu, Y., Ji, J., Cui, F., Sun, J., Wu, H., Pi, F., Zhang, Y., Sun, X., 2019b. Development of a two-step immunochromatographic assay for microcystin-LR based on fluorescent microspheres. Food Control 95, 34–40.

Ma, J., Yan, F., Chen, F., Jiang, L., Li, J., Chen, L., 2015. C_{18}-functionalized magnetic silica nanoparticles for solid phase extraction of microcystin-LR in reservoir water samples followed by HPLC-DAD determination. J. Liq. Chromatogr. Relat. Technol. 38 (6), 655–661.

Nameghi, M.A., Danesh, N.M., Ramezani, M., Alibolandi, M., Abnous, K., Taghdisi, S.M., 2019. An ultrasensitive electrochemical sensor for 17β-estradiol using split aptamers. Anal. Chim. Acta 1065, 107–112.

Que, H., Yan, X., Guo, B., Ma, H., Wang, T., Liu, P., Gan, X., Yan, Y., 2019. Terminal deoxynucleotidyl transferase and rolling circle amplification induced G-triplex formation: a label-free fluorescent strategy for DNA methyltransferase activity assay. Sens. Actuators B Chem. 291, 394–400.

Saberi, Z., Rezaei, B., Ensafi, A.A., 2019. Fluorometric label-free aptasensor for detection of the pesticide acetamiprid by using cationic carbon dots prepared with cetrimonium bromide. Microchimica Acta 186 (5).

Taghdisi, S.M., Danesh, N.M., Nameghi, M.A., Ramezani, M., Alibolandi, M., Abnous, K., 2019. An electrochemical sensing platform based on ladder-shaped DNA structure and label-free aptamer for ultrasensitive detection of ampicillin. Biosens. Bioelectron. 133, 230–235.

Taghdisi, S.M., Danesh, N.M., Ramezani, M., Abnous, K., 2016. A novel M-shape electrochemical aptasensor for ultrasensitive detection of tetracyclines. Biosens. Bioelectron. 85, 509–514.

Taghdisi, S.M., Danesh, N.M., Ramezani, M., Abnous, K., 2018. A new amplified fluorescent aptasensor based on hairpin structure of G-quadruplex oligonucleotide-Aptamer chimera and silica nanoparticles for sensitive detection of aflatoxin B_1 in the grape juice. Food Chem. 268, 342–346.

Taghdisi, S.M., Danesh, N.M., Ramezani, M., Ghows, N., Mousavi Shaegh, S.A., Abnous, K., 2017. A novel fluorescent aptasensor for ultrasensitive detection of microcystin-LR based on single-walled carbon nanotubes and dapoxyl. Talanta 166, 187–192.

Tang, Y., Chai, Y., Liu, X., Li, L., Yang, L., Liu, P., Zhou, Y., Ju, H., Cheng, Y., 2018. A photoelectrochemical aptasensor constructed with core-shell CuS-TiO2 heterostructure for detection of microcystin-LR. Biosens. Bioelectron. 117, 224–231.

Tong, P., Zhang, L., He, Y., Tang, S., Cheng, J., Chen, G., 2010. Analysis of microcystins by capillary zone electrophoresis coupling with electrospray ionization mass spectrometry. Talanta 82 (4), 1101–1106.

Wang, Y., Yang, L., Li, N., Sun, C., Xia, Y., Yuan, L., Lu, J., Liu, F., Xing, X., 2019. A versatile assay for alkaline phosphatase detection based on thymine-HgII-thymine structure generation mediated by TdT. Talanta 195, 566–572.

Welten, R.D., Meneely, J.P., Elliott, C.T., 2019. A Comparative Review of the Effect of Microcystin-LR on the Proteome. Expo. Health. https://doi.org/10.1007/s12403-019-00303-1.

Wu, Z., He, D., Cui, B., Jin, Z., 2019. Ultrasensitive detection of microcystin-LR with gold immunochromatographic assay assisted by a molecular imprinting technique. Food Chem. 283, 517–521.

Yang, P., Wang, X., Gu, Z., Li, H., Chen, D.D.Y., Yang, X., 2019. Evaluation of the binding of natural products with thrombin binding aptamer G-quadruplex using electrospray ionization mass spectrometry and spectroscopic methods. Talanta 200, 424–431.

Yang, R., Song, D., Fang, S., Liu, Y., Zhou, X., Long, F., Zhu, A., 2018. Development of novel portable and reusable fiber optical chemiluminescent biosensor and its application for sensitive detection of microcystin-LR. Biosens. Bioelectron. 121, 27–33.

Zastepa, A., Pick, F.R., Blais, J.M., Saleem, A., 2015. Analysis of intracellular and extracellular microcystin variants in sediments and pore waters by accelerated solvent extraction and high performance liquid chromatography-tandem mass spectrometry. Anal. Chim. Acta 872, 26–34.

Zhang, G., Li, C., Wu, S., Zhang, Q., 2018a. Label-free aptamer-based detection of microcystin-LR using a microcantilever array biosensor. Sens. Actuators B Chem. 260, 42–47.

Zhang, H., Luo, F., Wang, P., Guo, L., Qiu, B., Lin, Z., 2019a. Signal-on electrochemiluminescence aptasensor for bisphenol A based on hybridization chain reaction and electrically heated electrode. Biosens. Bioelectron. 129, 36–41.

Zhang, K., Ma, H., Yan, P., Tong, W., Huang, X., Chen, D.D.Y., 2018b. Electrochemical detection of microcystin-LR based on its deleterious effect on DNA. Talanta 185, 405–410.

Zhang, R., Sun, J., Ji, J., Pi, F., Xiao, Y., Zhang, Y., Sun, X., 2019b. A novel "OFF-ON" biosensor based on nanosurface energy transfer between gold nanocrosses and graphene quantum dots for intracellular ATP sensing and tracking. Sens. Actuators B Chem. 282, 910–916.

Zhang, W., Jia, B., Furumai, H., 2018c. Fabrication of graphene film composite electrochemical biosensor as a pre-screening algal toxin detection tool in the event of water contamination. Sci. Rep. 8 (1).

Zhang, Y., Zhu, Z., Teng, X., Lai, Y., Pu, S., Pang, P., Wang, H., Yang, C., Barrow, C.J., Yang, W., 2019c. Enzyme-free fluorescent detection of microcystin-LR using hairpin DNA-templated copper nanoclusters as signal indicator. Talanta 202, 279–284.